

1  
2  
3  
4  
5  
6  
7  
8  
9  
10  
11  
12  
13  
14  
15  
16  
17  
18  
19  
20  
21  
22  
23  
24

**The Double ITCZ Syndrome in GCMs: A Coupled Feedback Problem  
among Convection, Clouds, Atmospheric and Ocean Circulations**

Guang J. Zhang, Xiaoliang Song

Scripps Institution of Oceanography

La Jolla, CA 92093-0230

&

Yong Wang

Department of Earth System Science

Tsinghua University, Beijing, China 100084

Submitted to Atmospheric Research

December 30, 2018

Revised June 2, 2019

Corresponding author: Guang J. Zhang, Scripps Institution of Oceanography, La Jolla, CA  
92093-0230, Email: [gzhang@ucsd.edu](mailto:gzhang@ucsd.edu)

## Abstract

The appearance of a spurious double ITCZ south of the equator in coupled general circulation models has been a stubborn problem ever since the beginning of coupled model development. This article reviews the past research in this area, with a focus on three possible major contributors to the double ITCZ biases: 1) the southeastern Pacific marine stratus clouds and associated warm sea surface temperature (SST) biases; 2) the extratropical shortwave absorption biases over Southern Ocean; and 3) convective parameterization. The negative biases in marine boundary layer clouds in the southeastern Pacific lead to warm SST biases. Through coupled atmosphere-ocean interactions, it contributes to the double ITCZ bias. Positive shortwave absorption biases over Southern Ocean is believed to be an extratropical contributor to the double ITCZ biases in models. Since the heat from excess shortwave absorption must be transported to the northern hemisphere by the Hadley circulation, the position of the ITCZ must shift southward. However, later research finds that reducing the extratropical shortwave absorption has little effect on the ITCZ position. One possibility is that some feedback mechanism involving subtropical low-level clouds as intermediary is missing. For convective parameterization, changes in various elements in convection schemes can have large impacts on the ITCZ simulation. It involves a complex chain of interactions among convection, large-scale atmospheric circulation, SST, and upper ocean circulation. In one scheme, changes in the scheme lead to the elimination of double ITCZ in all seasons, giving hope that we can finally take on the double ITCZ problem.

## 47 **1. Introduction**

48           The latent heat release from tropical precipitation is an important energy source for driving  
49 the atmospheric circulation. A major feature of the climatological mean tropical precipitation  
50 distribution is a strong band of precipitation that appears north of the equator year-round,  
51 particularly in the Pacific, in spite of the fact that the annual mean downward solar radiation is  
52 symmetric about the equator. This is largely due to the asymmetric distribution of landmasses  
53 between the northern and southern hemispheres, combined with the wind-evaporation- sea surface  
54 temperature (SST) feedbacks (Xie and Philander 1994). While observations show a single  
55 precipitation band north of the equator except in boreal spring when a secondary precipitation band  
56 also appears south of the equator in the central and eastern equatorial Pacific (Zhang, 2001),  
57 coupled general circulation models (CGCMs), on the other hand, show two nearly zonally parallel  
58 precipitation bands straddling the equator, the so-called double intertropical convergence zone  
59 (ITCZ). The annual mean precipitation bias in the southern ITCZ region is also accompanied by  
60 warm biases of SST and anomalous convergence of wind stress.

61           This double ITCZ problem has plagued generations of CGCMs for more than two decades  
62 (Mechozo et al., 1995; Lin, 2007; Zhang et al., 2015). Even in the latest version of global climate  
63 models and Earth system models, e.g. those that participated in the Inter-governmental Panel on  
64 Climate Change (IPCC) AR5, double-ITCZ remains one of the most common problems among  
65 the models (Zhang et al. 2015). In spite of the fact that extensive work has been done to understand  
66 the causes of the double ITCZ problem, progress has been very slow in this area. The atmospheric  
67 general circulation models (AGCMs) forced with observed SSTs typically exhibit weak double  
68 ITCZ biases, but they are severely exacerbated in corresponding CGCMs, indicating that air-sea  
69 interaction and simulated SST biases play important roles in the formation of double ITCZ biases.

70 Many studies have been devoted to understanding the air-sea feedback mechanisms and  
71 the causes of SST biases related to the double ITCZ bias. Mechoso and Ma (1995) analyzed 11  
72 CGCMs and found that all models that have double ITCZ biases also have negative biases in  
73 stratocumulus clouds and warm SST biases in southeastern Pacific (SEP) off the coast of Peru.  
74 They suggested that lack of sufficient low-level clouds in the SEP region was at least partly  
75 responsible for the warm SST biases, which in turn contribute to the double ITCZ bias.

76 While the marine boundary layer low-level clouds in SEP represent subtropical influence  
77 on the formation of double ITCZ, extratropical cloud influence on the double ITCZ has also been  
78 studied extensively from the energetics point of view (Kang et al. 2008, Kang et al. 2009, Hwang  
79 and Frierson 2013). Hwang and Frierson (2013) argued that negative biases in cloud simulation in  
80 the Southern Ocean allows the southern hemisphere to receive more energy than it should. To get  
81 rid of this excess energy, the Hadley circulation has to have stronger upward motion south of the  
82 equator and downward motion north of the equator, thereby facilitating cross-equatorial energy  
83 transport in the upper troposphere. This creates the southern ITCZ in GCMs. Other studies along  
84 this line of research (e.g., Kay et al. 2016, Hawcroft et al. 2017), however, found that the Southern  
85 Ocean cloud problem had little effect on tropical ITCZ if the oceanic cross-equatorial heat  
86 transport is taken into account.

87 As ITCZ precipitation is mostly of convective nature, it is natural to suspect that convective  
88 parameterization is a major factor responsible for double ITCZ biases. Chao and Chen (2001)  
89 carried out a theoretical study, arguing that the ITCZ is a tug of war between the Coriolis factor  
90 and SST. In their idealized numerical experiments, they found that a single or a double ITCZ can  
91 form, depending on the convective parameterization scheme used. Zhang and Wang (2006)  
92 modified the Zhang-McFarlane scheme (Zhang and McFarlane 1995) in the National Center for

93 Atmospheric Research (NCAR) Community Climate System Model (CCSM3) and showed that it  
94 had a significant impact on the ITCZ simulation. Song and Zhang (2009) and Zhang and Song  
95 (2010) analyzed the interaction mechanisms both within the atmosphere and between atmospheric  
96 and oceanic processes. They showed that convective parameterization affects the simulation of  
97 ITCZ through a chain of complex interactions involving atmospheric processes, atmosphere-ocean  
98 coupling and upper ocean heat transport. Other diagnostic studies were also actively pursued to  
99 identify mechanisms responsible for the double ITCZ biases in GCMs (Lin 2007, Bellucci et al.  
100 2010, Uoeslati and Bellon 2015).

101 This paper reviews the double ITCZ problem and progress made in the past two decades.  
102 Section 2 will be devoted to the role of southeastern Pacific climate in ITCZ simulation. Section 3  
103 will review the roles of extratropical biases and cross-equatorial energy transport in ITCZ  
104 simulation. Section 4 will present recent progress in mitigating the double ITCZ biases through  
105 improving elements in convective parameterization and related moist processes. Section 5 will  
106 summarize the paper and provide some discussions.

## 107 **2. The southeastern Pacific cloud and SST problem**

108 The double ITCZ problem had been in existence ever since the early days of coupled ocean-  
109 atmosphere model development. The double ITCZ bias was first reported in a paper resulting from  
110 meetings of the early CGCMs practitioners (Mechoso et al. 1995). At the time, the need for the  
111 CGCMs was argued on the basis of the demand for climate forecasts at time scales in which SSTs  
112 can no longer be prescribed (Mechoso 2019, personal communication). Mechoso et al. (1995)  
113 examined 11 CGCMs and found that all models exhibit a double ITCZ problem in the eastern  
114 Pacific, either in the form of two precipitation bands straddling the equator year-round or an ITCZ  
115 that migrates across the equator following the seasonal cycle, with a strong precipitation band

116 located south of the equator from January to June and north of the equator from July to December.  
117 The cold tongue over the equator is too strong and extends too far west. They noted that marine  
118 stratocumulus clouds off the Peruvian coast in the models were seriously underestimated. This  
119 would produce a wrong feedback between marine boundary layer clouds and the underlying ocean.  
120 Thus, deficient marine stratus clouds in SEP were suspected to be among factors responsible for  
121 the warm SST biases in the region, and therefore a contributing factor to the double ITCZ problem.  
122 Ma et al. (1996) investigated this notion by prescribing a stratus cloud cover, constant in time, off  
123 the Peruvian coast in a CGCM. They found that SSTs in the SEP were indeed better simulated,  
124 and precipitation simulation south of the equator in the eastern Pacific was also improved. The  
125 SSTs underneath the prescribed cloud cover are decreased by as much as 5 K due to reduced solar  
126 radiation. There is also large cooling elsewhere south of the equator and in the cold tongue in the  
127 eastern and central Pacific. Away from the prescribed cloud deck region on the equator side, the  
128 southeasterly winds are enhanced due to strengthened SST gradient and associated surface  
129 pressure gradient. This increases the evaporative cooling of the ocean surface. In the equatorial  
130 cold tongue region, enhanced cold water advection westward makes the simulation of the  
131 equatorial cold tongue worse. Yu and Mechoso (1999) further investigated the Peruvian stratus  
132 effect on SST in the eastern equatorial Pacific by including its annual variation when prescribing  
133 the stratus cloud cover off the Peruvian coast. They found that the annual variation of the stratus  
134 clouds plays an important role in the annual variation of the equatorial cold tongue.

135 Gordon et al. (2010) performed a set of similar experiments using the GFDL CGCM by  
136 prescribing climatological monthly mean low cloud cover from ISCCP observations. They found  
137 that while in the standard GFDL CGCM there were large negative biases in SEP stratus and  
138 positive SST biases underneath, with prescribed low clouds from ISCCP the warm SST biases in

139 SEP region were greatly reduced and the spatial distribution of SST became more asymmetric  
140 about the equator. The cloud-induced local cooling from reduced shortwave radiation enhances  
141 the dynamical cooling from southeasterly trade winds. As a result, there are much stronger  
142 southeasterly trade winds in the region and the eastern equatorial Pacific cold tongue becomes  
143 colder. The intensified cold tongue also has a large impact on ENSO simulation in their model,  
144 inhibiting eastward progression of warm water to the east of dateline.

145         The simulation of marine stratus clouds in the SEP region is still problematic in current  
146 GCMs. Fig. 2 shows the annual mean low-cloud fraction and surface shortwave cloud radiative  
147 forcing (SWCRF) in the region from CALIPSO observations and AMIP simulations of the models  
148 that participated in the CMIP5 model intercomparison project. The models seriously under-  
149 simulate the stratus fraction. Observations show cloud fraction as high as 80% off the coast of Peru  
150 while models show less than 40%. As a result, the surface SWCRF is also underestimated: the  
151 CERES-EBAF observed SWCRF is as much as  $-85 \text{ Wm}^{-2}$  as compared to about  $-55 \text{ Wm}^{-2}$  in  
152 models. The excessive shortwave radiation into the ocean surface due to the lack of sufficient low-  
153 level clouds would lead to warm SST biases in CGCMs.

154         One link between the marine boundary layer stratus off the Peruvian coast and the double  
155 ITCZ in the eastern Pacific is that the stratus cloud reduces SSTs underneath it. When there are  
156 more low clouds in the SEP region the SSTs underneath decrease. The colder SST leads to lower  
157 near-surface air temperature and thus higher atmospheric pressure under hydrostatic  
158 approximation. The resulting pressure gradient generates the southeasterly trade winds. The  
159 dynamical cooling due to coastal upwelling and surface evaporative cooling increases. The SST  
160 cooling further leads to more stratus clouds, which in turn reduces surface solar radiation and  
161 increases cloud top longwave cooling, both of which enhance the southeasterly winds (Nigam

162 1997). The stronger southeasterly winds push the cold water to the northwest, expanding the cold  
163 SST region. The northwestward ocean surface current advects cold water into the central Pacific  
164 south of the equator, keeping SSTs in check and thereby suppressing convection there. In  
165 consideration of this chain of interactions, through which the eastern Pacific double ITCZ biases  
166 may be alleviated, Song and Zhang (2016) directly prescribed SSTs in the SEP (5°S-25°S, 120°W  
167 to Peruvian coast) to determine the degree to which the double ITCZ problem is affected by the  
168 warm SST biases in the SEP. Fig. 3 shows the annual mean precipitation distribution from GPCP  
169 observations, the fully coupled simulation (CNTL) from NCAR CESM1 and the coupled  
170 simulation with SSTs in the SEP region prescribed (also referred to as SEP run), and their  
171 differences. Compared to GPCP observations, the standard CESM1 simulates too much  
172 precipitation south of the equator east of the dateline all the way to the Peruvian coast by 3 to 5  
173 mm day<sup>-1</sup>. In the equatorial region, there is a dry tongue near the dateline and to its west (130°E)  
174 in the warm pool, corresponding to the westward extension of the cold tongue. On the other hand,  
175 in the eastern Pacific cold tongue region, the model precipitation field has positive biases. The  
176 northern ITCZ precipitation is also overestimated. When SSTs in the SEP are prescribed to  
177 observed values, although the double ITCZ remains to exist, the magnitude of the precipitation  
178 biases is reduced throughout the southeastern and central Pacific south of the equator east of the  
179 dateline. In the equatorial region, both the wet bias east of the dateline and the dry bias in the warm  
180 pool are reduced to a level in much closer agreement with observed precipitation. However, the  
181 positive biases in the northern ITCZ are increased.

182 Song and Zhang (2016) carried out further analysis and showed that changes in  
183 precipitation distribution from the fully coupled simulation to the one with SSTs in the SEP region  
184 prescribed involve a series of atmosphere-ocean interactions. They found that when SSTs in SEP



185 are prescribed, the colder SST suppresses convection and precipitation locally. In addition, the  
186 colder SST leads to higher surface pressure, and the resulting pressure gradient force induces the  
187 southeasterly winds outside the prescribed SST region, cooling the ocean via increased evaporation.  
188 Convection in the eastern Pacific is suppressed, which enhances the Walker circulation and  
189 increases the easterly winds in the lower troposphere of the equatorial region. This enhances the  
190 equatorial upwelling and shoals the thermocline over the eastern Pacific. The changes of surface  
191 wind stress and its associated wind stress curl also modify the upper ocean currents, preventing  
192 the warm water in the western Pacific from expanding eastward. As a result of these interaction  
193 processes in the atmosphere and the ocean, the double-ITCZ bias and the dry equator cold tongue  
194 bias are both improved.

195         The tropical North Atlantic ( $5^{\circ}\text{N}$ - $25^{\circ}\text{N}$ , hereafter referred to as TNA) SST biases in GCMs  
196 were also believed to contribute to the eastern Pacific double ITCZ biases either directly or  
197 indirectly (Wang et al. 2014, Zhang et al. 2014, Song and Zhang 2017). Wang et al. (2014) showed  
198 that among 22 CMIP5 models cold SST biases in TNA are highly correlated with warm SST biases  
199 in the SEP. Zhang et al. (2014) performed a sensitivity experiment using the NCAR CESM1 to  
200 determine how TNA SST could affect the SEP SST. They found that cold SST biases in the TNA  
201 weakens the local Hadley-type circulation, which has its ascending branch in the TNA and  
202 descending branch in the SEP. The weakened subsidence in the SEP reduces low-level stratus  
203 cloud cover, thereby leading to warm SST biases there.

204         Song and Zhang (2017) also conducted an investigation on this by performing an  
205 experiment using NCAR CESM1 similar to that in Song and Zhang (2016), except by prescribing  
206 SSTs either in TNA, SEP, or combined. They found that prescribing SST in TNA only has a slight  
207 cooling effect on the SEP SST. However, it does reduce precipitation in the southern ITCZ and

208 increase precipitation in the northern ITCZ in the eastern Pacific, particularly when combined with  
209 prescribing the SEP SST. The removal of cold SST biases in the TNA leads to southwesterly wind  
210 anomalies near the surface in the northern ITCZ region and southeasterly wind anomalies in the  
211 SEP. These wind anomalies, when superposed with the prevailing northeasterly in the northern  
212 ITCZ region and southeasterly in the SEP, warm the ocean surface north of the equator and cool  
213 the ocean surface in the SEP through changes in surface latent heat flux. The low-level wind  
214 changes also lead to changes in low-level mass and moisture convergence, increasing precipitation  
215 in the northern ITCZ and decreasing precipitation in the southern ITCZ region (Fig. 4).

216 Song and Zhang (2019) further analyzed the NCAR CESM1 simulation of precipitation for  
217 boreal spring in the eastern Pacific. They showed that the seasonally alternating double ITCZ in  
218 boreal spring can be traced back to positive precipitation and cold SST biases in the northern ITCZ  
219 in the eastern Pacific during boreal winter. The cold SST biases persist to boreal spring and  
220 suppress convection in the northern ITCZ region. The moisture is transported by the northeasterly  
221 trade winds across the equator to the south, leading to enhanced precipitation in the southern ITCZ  
222 region.

223 To summarize, CGCMs under-simulate marine boundary layer stratus clouds and produce  
224 warm SST biases in the SEP region. Failure to capture the ocean-atmosphere feedbacks involving  
225 marine stratus clouds is one of the contributors to the double ITCZ problem in the central and  
226 eastern Pacific south of the equator. Cold SST biases in the TNA also contribute to the problem  
227 by either affecting stratus cloud cover and thus SSTs in the SEP region or the lower tropospheric  
228 circulation and moisture convergence in the northern ITCZ in the eastern Pacific. SST biases in  
229 the northern ITCZ in boreal fall and winter also affect the double ITCZ in boreal spring south of  
230 the equator. All these are contributing factors to the double ITCZ problem.

### 231 3. The Southern Ocean shortwave absorption problem

232 While the SEP stratus cloud problem is a relatively local (i.e. tropical and subtropical)  
233 contributor to the double ITCZ bias, non-local contributors have also been sought. Based on  
234 theoretical energetics analysis and idealized GCM experiments, Kang et al. (2008) demonstrated  
235 that ITCZ would shift towards the hemisphere that is heated more at the surface or top of  
236 atmosphere, and that extratropical clouds could be important for the tropical ITCZ location. As a  
237 result of this energetics argument, Hwang and Frierson (2013) recently proposed that Southern  
238 Ocean model cloud biases in coupled GCMs could be responsible for the double ITCZ biases.  
239 They analyzed 20 CMIP5 CGCMs and found that cross-equatorial energy transport is highly  
240 correlated with the double ITCZ biases in the models: the larger the energy transport from southern  
241 hemisphere to northern hemisphere, the more serious the double ITCZ problem in a model. They  
242 further showed that cloud biases over the Southern Ocean are a major contributor to biases in  
243 cross-equatorial energy transport. Based on these analyses, they posited the following feedback  
244 mechanism that links the Southern Ocean cloud bias to the ITCZ bias in the tropics: The negative  
245 biases in cloud cover over the Southern Ocean leads to more absorption of shortwave radiation at  
246 the top of the atmosphere. The excess energy from this in the southern hemisphere must be  
247 transported to the northern hemisphere by enhanced upper branch of the Hadley circulation. As a  
248 response, the ascending branch of the Hadley cell moves to the south of the equator, leading to the  
249 southward shift of the ITCZ and creating the double ITCZ problem.

250 The above proposed feedback mechanism ignored the ocean's role in the cross-equatorial  
251 heat transport. Kay et al. (2016) designed a coupled model simulation experiment to test this  
252 hypothesis. They used the NCAR CESM1, which does have a prominent double ITCZ problem as  
253 well as a strong negative bias in cloud optical properties over the Southern Ocean. By artificially

254 increasing the amount of supercooled cloud liquid water in low-level clouds over the Southern  
255 Ocean, they found that the absorbed shortwave radiation bias in the atmosphere was reduced.  
256 Consequently, the northward cross-equatorial energy transport was also reduced. However, much  
257 (80%) of the reduction was accomplished by the ocean and the atmospheric transport only accounts  
258 for 20% of the change, and there was little change in the double ITCZ bias. Their results suggest  
259 that when dynamic ocean heat transport is included, the influence of Southern Ocean cloud  
260 simulation on ITCZ through the proposed mechanism by Hwang and Frierson (2013) is limited.  
261 Kay et al. (2016) also ran a simulation with the atmospheric model coupled with a slab ocean  
262 model, in which the ocean heat transport was prescribed and fixed. They found that in this case  
263 indeed the reduction of northward cross-equatorial energy transport was accomplished through the  
264 atmosphere, the southern ITCZ precipitation was reduced and the northern ITCZ precipitation was  
265 increased, consistent with the results of Hwang and Frierson (2013). Their results are schematically  
266 synthesized in Fig. 5. When there is more supercooled cloud liquid water in the Southern Ocean  
267 low-level clouds, in the extratropics less solar radiation is absorbed at the top of the atmosphere  
268 and the atmospheric zonal circulation is modified. In the tropics, if the atmosphere is to take all  
269 the burden of energy transport, it will increase the southward (or, relatively, decrease the northward)  
270 energy transport across the equator by the upper branch of the Hadley circulation, which  
271 suppresses the southern ITCZ and enhances the northern ITCZ. If the ocean heat transport is  
272 allowed, much of the required extra cross-equatorial heat transport will be accomplished through  
273 the ocean and little adjustment is needed in the atmosphere. For details, see Kay et al. (2016).

274         Increasing supercooled cloud liquid water over the Southern Ocean is one way to reduce  
275 the shortwave absorption there. Another way is to reduce ocean surface albedo. Hawcroft et al.  
276 (2017) performed such an experiment using the UK Met Office Hadley Centre GCM HadGEM2-

277 ES. In a series of CGCM simulations they modified surface albedo in both hemispheres to give an  
278 interhemispheric albedo difference approaching the observed difference. While the total cross-  
279 equatorial energy transport was improved, the double ITCZ problem that existed in the model did  
280 not improve, and in fact became worse. Similar to Kay et al. (2016), Hawcroft et al. (2017) also  
281 found that most of the cross-equatorial energy transport was accomplished by the ocean, not the  
282 atmosphere. Hawcroft et al. (2018) recently further experimented with the HadGEM2-ES by  
283 perturbing energy input into the Earth system at different latitudes to investigate this issue. By  
284 modifying stratospheric aerosols that reflect incoming solar radiation in the model, they found that  
285 the impacts on tropical climate of high and low latitude forcing are very different, with large  
286 changes in tropical precipitation and double ITCZ when the tropics are cooled. When the  
287 extratropics are cooled, the tropical precipitation response is weak. Using different methods to  
288 perturb the absorbed shortwave radiation at the surface or top-of-atmosphere and different GCMs,  
289 both Kay et al. (2016) and Hawcroft et al. (2017, 2018) reach the same conclusion that reducing  
290 Southern Ocean biases will not improve the atmospheric cross-equatorial energy transport and will  
291 not improve the double ITCZ problem either.

292 Green and Marshall (2017) also performed a CGCM experiment using the MITgcm, in  
293 which they imposed an interhemispheric albedo contrast and examined how the ocean circulation  
294 responds to it through cross-equatorial energy transport and associated energy fluxes, thereby  
295 affecting the ITCZ's position. They found that the ITCZ's response to the imposed  
296 interhemispheric heating contrast was strongly damped by the trade-wind driven ocean circulation  
297 through its coupling with the Hadley circulation in the atmosphere. Similar to Kay et al. (2016)  
298 and Hawcroft et al. (2017), they conclude that the position of ITCZ is much less sensitive to  
299 interhemispheric heating contrasts than previously thought. These works together provides strong

300 evidence to refute the link between the Southern Ocean bias and the double ITCZ bias in GCMs  
301 as proposed by Hwang and Frierson (2013).

302 In light of the work of Kay et al. (2016) and Hawcroft et al. (2017), Schneider (2017)  
303 developed a theoretical framework under which both atmospheric and oceanic energy transports  
304 are considered. Assuming that oceanic energy transport is accomplished by Ekman mass flux in  
305 the upper ocean due to Ekman coupling with the atmosphere via surface wind stress, he showed  
306 that to first order approximation the response of atmospheric cross-equatorial energy transport to  
307 perturbations in energy input into the atmosphere in the Southern Ocean is weaker by a factor of  
308 3 when cross-equatorial oceanic energy transport is considered. This is consistent with the work  
309 of Kay et al. (2016), Hawcroft et al. (2017) and Green and Marshall (2017) and reconciles the  
310 difference between these works and that of Hwang and Frierson (2013).

311 Before concluding this section, we note that Mechoso et al. (2016) also carried out a  
312 sensitivity experiment to investigate the impact of altered shortwave radiation input into the  
313 atmosphere-ocean system in the Southern Ocean on double ITCZ in the tropics. In an idealized  
314 simulation using two different GCMs, one being the UCLA GCM and the other being NorESM, a  
315 Norwegian version of the NCAR CESM1, the shortwave radiative flux at the top of the model in  
316 the latitude belt of 30°S-60°S was reduced by an amount comparable to model biases there. They  
317 found that the response of the ITCZ position in UCLA GCM was strong, with the southern ITCZ  
318 weakened significantly, whereas the response in the NorESM was quite weak, with little change  
319 in the southern ITCZ. In an essence, the UCLA GCM qualitatively agrees with the argument of  
320 Hwang and Frierson (2013) and the NorESM agrees with the results of Kay et al. (2016) and others.  
321 They further analyzed the feedback between SST and stratocumulus in the subtropical cold waters  
322 off the west coast of major continents (i.e. Peruvian, Angolan and Californian stratus decks) and

323 found that this feedback played an important role in the different response of the two GCMs. The  
324 UCLA GCM has a strong feedback between the stratus cloud decks and the underlying SST  
325 whereas the NorESM does not. The extratropical cooling in SST due to reduced solar radiation  
326 absorption leads to enhanced westerly winds, which when reaching the west coasts of the  
327 continents turn to become southerlies to the subtropics. This induces coastal upwelling and cools  
328 the local SST, which triggers the SST-stratus feedback to produce more marine stratus clouds,  
329 further cooling the ocean surface below the subtropical stratus region. Through the mechanisms  
330 discussed in Section 2, cooling of southeastern Pacific SST reduces the double ITCZ bias south of  
331 the equator in tropical eastern and central Pacific. This offers a new perspective on how  
332 extratropical biases can affect the tropical ITCZ bias; and it depends on the atmospheric circulation,  
333 subtropical marine stratus and SST feedback as an intermediary. In particular, it raises the  
334 possibility that the extratropical influence on tropical climate may critically depend on other  
335 feedback mechanisms being properly represented in CGCMs.

336 To summarize, extratropical biases in cloud simulation in the Southern Ocean were  
337 suggested to be a main contributor to the double ITCZ problem in the tropics. This was based on  
338 energetics argument that the hemisphere that receives excess energy must get rid of it through  
339 cross-equatorial energy transport by the upper branch of the Hadley circulation. As a result, the  
340 ITCZ, which is the ascending branch of the Hadley circulation, would move toward the hemisphere  
341 that has excess energy input. However, the argument neglected energy transport by the oceans.  
342 When the ocean response to energy perturbation in the extratropics is included, 70 to 80% of the  
343 required cross-equatorial energy transport is accomplished by the oceans. Thus, the ITCZ response  
344 is largely muted. A new perspective, though, is that it may depend on stratocumulus cloud feedback  
345 to SST in subtropical cold waters off the west coast of continents. This deserves further

346 investigation. An Extratropical-Tropical Interaction model intercomparison project is being  
347 planned currently to investigate how tropical climate responds to extratropical forcing (Mechoso  
348 2019, personal communication).

#### 349 **4. The convection parameterization problem**

350 The ITCZ is a region of active deep convection. Therefore, it is natural to seek answers to  
351 the double ITCZ problem in convection parameterization in GCMs. Chao and Chen (2001)  
352 suggested that the position of ITCZ is determined by two competing factors, the Earth's rotation  
353 factor, i.e. the Coriolis force, that attracts the ITCZ to the equator (since damping of  
354 convergence/divergence perturbations is proportional to the Coriolis parameter and thus is the least  
355 at the equator), and surface turbulent fluxes from the rotational flow induced by convergence in  
356 high SST regions off the equator due to Coriolis deflection that pulls the ITCZ from the equator.  
357 They demonstrated that convective parameterization schemes could produce either a single ITCZ  
358 or a double ITCZ.

359 The double ITCZ precipitation bias often exists in atmospheric model simulations forced  
360 with observed SSTs and becomes more serious in the corresponding fully-coupled simulations.  
361 This indicates that convection parameterization can be responsible for the double ITCZ  
362 precipitation bias in stand-alone atmospheric GCMs and the coupled feedbacks play important  
363 roles in amplifying the bias in CGCMs. Lin (2007) analyzed the ocean-atmosphere feedbacks  
364 related to the double ITCZ problem in the coupled GCMs participating in the IPCC AR4. He  
365 identified that excessive sensitivity of precipitation to SST is a common bias in many GCMs and  
366 suggested that suppressing deep convection and decoupling it from SST by including some  
367 negative feedback mechanisms in convection parameterization schemes could alleviate the double  
368 ITCZ bias.



369 Bellucci et al. (2010) analyzed the relationship between the double ITCZ biases and the  
370 representation of large-scale vertical motion regime in IPCC AR4 CGCMs. Using a regime sorting  
371 approach first proposed by Bony et al. (2004), they showed that the double ITCZ bias was mostly  
372 due to overly frequent occurrence of deep convection regime associated with strong upward  
373 motion. They further analyzed the relationship between SST and the onset of convection in the  
374 models over the southern ITCZ region and found that models that have lower SST threshold for  
375 convection onset relative to the most frequently occurring SST in the region generally have more  
376 severe double ITCZ biases. Ouselati and Bellon (2015) further explored the interaction between  
377 SST, large-scale atmospheric circulation and the double ITCZ and proposed a process-oriented  
378 diagnostic metric to quantify this interaction using precipitation bias in each vertical motion regime.  
379 All these studies point to the important role of deep convection in the double ITCZ biases in  
380 CGCMs.

381 Several studies have attempted to mitigate the double ITCZ bias by improving convection  
382 parameterization schemes to reduce precipitation bias and reduce the sensitivity of convection to  
383 SST. Zhang and Wang (2006) investigated the effect of convective parameterization on ITCZ  
384 simulation in the NCAR CCSM3. In the model, convection is parameterized using the ZM scheme,  
385 which uses the consumption of convective available potential energy (CAPE) as a closure to  
386 determine the amount of convection, given large-scale atmospheric state. Since CAPE is largely  
387 determined by thermodynamic instability associated with local SST, this CAPE-based closure  
388 generally leads to high sensitivity of convection to SST. Zhang and Wang (2006) replaced the  
389 CAPE-based closure with one based on large-scale CAPE generation in the free troposphere  
390 following Zhang (2002), which is derived from the analysis of observational data from the  
391 Atmospheric Radiation Measurement (ARM) program, in the ZM convection scheme. The

392 convection parameterized by the new closure is largely controlled by large-scale forcing in the free  
393 troposphere, resulting in a lower sensitivity of convection to SST and better precipitation  
394 simulation in the atmospheric model (Zhang and Mu 2005, Song and Zhang 2009). The coupled  
395 simulation of Zhang and Wang (2006) shows that precipitation bias in the southern ITCZ region  
396 is almost entirely eliminated in boreal summer and fall with the modified ZM convection scheme  
397 (Fig. 6), although biases still persist in boreal winter and spring. This demonstrates that improving  
398 convective parameterization schemes is an effective way to address the double ITCZ problem in  
399 coupled GCMs.

400 To illustrate the impact of changing convective parameterization closure on the  
401 development of the spurious ITCZ, Fig. 7 shows 22-year-long time series of precipitation, SST  
402 and shortwave cloud forcing (SWCF) averaged in the southern ITCZ region ( $5^{\circ}\text{S}$ - $10^{\circ}\text{S}$ ,  $180^{\circ}\text{W}$ -  
403  $130^{\circ}\text{W}$ ) from the control run (CTRL) and the run (ICON) with the modified ZM convection  
404 scheme, respectively. Both runs start from a warm-start initial condition, as in Zhang and Wang  
405 (2006). At the end of year 11, the convection closures are switched between the two runs,  
406 everything else remaining unchanged. In the CTRL run, before the switch of closure, the average  
407 precipitation in the southern ITCZ region is above  $5 \text{ mm day}^{-1}$  year-round, with higher  
408 precipitation in boreal winter and spring and lower values in boreal summer and fall. In the ICON  
409 run, precipitation drops to  $1\sim 2 \text{ mm day}^{-1}$  in boreal summer and fall but remains more or less  
410 unchanged in boreal winter and spring from the CTRL run. The area-averaged SST in the CTRL  
411 run is systematically higher than in the ICON run year-round. Once the closures are switched, the  
412 time series patterns between CTRL and ICON are also switched, such that the run with CAPE-  
413 based closure always produces more precipitation and the run with large-scale CAPE generation  
414 closure always produces less precipitation in boreal summer and fall in the southern ITCZ region.

415 Note that the convection scheme influences the double ITCZ bias very quickly, within the first few  
416 months of the simulations. This experiment demonstrates unambiguously the role of convection  
417 closure in reducing the double ITCZ bias.

418 Further analyses (Song and Zhang, 2009) of the experiments show that in the simulation  
419 where the double ITCZ bias is reduced SST, wind stress, ocean thermocline, upper ocean currents,  
420 temperature and salinity are all systematically reduced. To understand how the modified  
421 convection scheme in the atmospheric model influences SST and ocean processes, Zhang and Song  
422 (2010) analyzed the coupled atmosphere-ocean feedback in the simulations with the modified  
423 convection scheme. They found that the reduction of SST bias in the southern ITCZ region is  
424 largely achieved by altering ocean dynamic heat transport, which is related to the upper ocean  
425 circulation change driven by changes in ocean surface wind stress associated with the modified  
426 convection. Their analyses suggest that the summer double ITCZ bias in the central Pacific  
427 southern ITCZ region in the CCSM3 is formed through a complex coupled feedback process that  
428 is triggered by unrealistically simulated convection in the atmospheric model.

429 Fig. 8 shows the schematic of the coupled feedback processes in the NCAR CCSM3 based  
430 on the work of Song and Zhang (2009) and Zhang and Song (2010). When the AGCM produces  
431 an initial positive precipitation bias in the southern ITCZ region in the central Pacific, the  
432 associated enhancement of surface wind convergence reduces the southeasterly trade winds west  
433 of the initial convection region. The reduced easterly will not only weaken the westward South  
434 Equatorial Current (SEC) but also result in much stronger negative wind stress curl, which will  
435 create oceanic upwelling below it, causing the thermocline to ridge (blue curve in the meridional  
436 cross section in Fig. 8a) through Ekman pumping and the sea level to dip (black curve in the  
437 meridional cross section part). The sloping sea level height north of it will in turn cause a south

438 equatorial countercurrent (SECC). The warm water from western Pacific can then be transported  
439 eastward to central and eastern Pacific by SECC, leading to warm SST bias, which can further  
440 strengthen convection. This feedback process can significantly amplify the convection bias in the  
441 southern ITCZ region and lead to a serious double ITCZ bias. This mechanism is similar to that  
442 proposed by Zhang et al. (2007). Zhang and Song (2010) attributed the wind stress curl bias to  
443 meridional changes of zonal wind stress, while Zhang et al. (2007) emphasized latitudinal changes  
444 of wind direction. In addition, the decrease of surface latent heat flux associated with the reduced  
445 easterly winds also contributes to the warm bias of SST, forming a convection-wind-evaporation-  
446 SST feedback. The revised convective closure tends to suppress convection in the southern ITCZ  
447 region in the central Pacific (Fig. 8b), thus moisture in the central Pacific can be transported  
448 westward to western Pacific by the easterly trade winds and fuel the deep convection in western  
449 Pacific, leading to a stronger Walker circulation and thus stronger easterly trade winds in the  
450 southern ITCZ region. The intensified easterly trade winds can suppress the aforementioned  
451 positive feedbacks of convection–wind–ocean current–SST and convection-wind-evaporation-  
452 SST, resulting in the mitigation of the double-ITCZ bias.

453         The suppression of the southern ITCZ also enhances the north-to-south asymmetry across  
454 the equator in the eastern and central Pacific. Fig. 9 shows the meridional cross section of the  
455 upper ocean temperature and zonal currents averaged over 180°E-150°W. In the CTL run, in  
456 response to the decrease of the easterly trade winds over the spurious southern ITCZ and the  
457 wind stress curl change as schematically shown in Fig. 8a, oceanic upwelling occurs from 13°S  
458 to 5°S, leading to thermocline ridging at 8°S. This drives an eastward SECC between 8°S and  
459 4°S. As a result, both upper ocean temperature and zonal currents are roughly symmetric about  
460 the Equator. By contrast, the simulation with the revised convection scheme only has a weak

461 thermocline ridge, which leads to a weak SECC between 4°S and 7°S below the sea surface.  
462 There is no significant thermocline ridge or SECC in GODAS observations (Fig. 9c). Both the  
463 simulation with the revised convection scheme and the GODAS observations show asymmetric  
464 distribution of thermocline and zonal currents.

465 In addition to convective parameterization closure, representation of processes in  
466 convection and other moist physics schemes are also investigated to identify their roles in ITCZ  
467 simulation. Bacmeister et al. (2006) found that weak rain re-evaporation also leads to double ITCZ.  
468 Using a NASA AGCM, they performed a series of experiments with increased fraction of rain re-  
469 evaporation, and showed that by increasing rain re-evaporation, the double ITCZ that exists in  
470 their atmospheric model can be largely eliminated. They further analyzed possible mechanisms  
471 responsible for this and found that the coupling between rain-related latent heating and boundary  
472 layer convergence at high frequency (periods less than about two weeks) is responsible for the  
473 double ITCZ. By increasing rain re-evaporation, associated stronger cooling from it in the  
474 boundary layer disrupt this coupling, thereby improving the ITCZ simulation.

475 Oueslati & Bellon (2013) performed several sensitivity experiments using a hierarchy of  
476 the French GCM Centre National de Recherches Météorologiques Coupled Global Climate Model,  
477 version 5.1 (CNRM-CM5.1) to investigate the effect of lateral entrainment in a convection scheme  
478 on double ITCZ bias. They show that increasing entrainment rates in convective parameterization  
479 can reduce the precipitation bias in the southern ITCZ region in their models. However, even with  
480 5 times of typical entrainment rates, the double ITCZ precipitation biases still persist in December–  
481 March.

482 Recently, Song and Zhang (2018) demonstrated that the double ITCZ biases in the NCAR  
483 CESM1 in all seasons, especially in boreal winter and spring, can be largely eliminated by

484 improving convection parameterization. All three components of the ZM convection scheme, i.e.,  
485 trigger function, closure assumption, and cloud model, were modified. The trigger function, which  
486 specifies the condition for convection onset, was determined by CAPE generation rate from large-  
487 scale forcing in the free troposphere based on systematical evaluation by Suhas and Zhang (2014),  
488 instead of CAPE as used in the original ZM scheme. Convection schemes commonly employ one-  
489 dimensional entraining plume cloud model to calculate convective transport of heat, moisture, and  
490 momentum. A simple bulk cloud model with constant lateral entrainment rate in height for each  
491 plume that forms the bulk model is used in the original ZM scheme for efficiency. However, a  
492 bulk cloud model is not able to represent various types of convective elements in a cumulus  
493 ensemble. Further, cloud-resolving model results show that entrainment rates usually vary with  
494 height, as shown in recent cloud resolving model studies (Gregory 2001, de Rooy et al. 2013,  
495 Zhang et al. 2016, and many others). The lateral entrainment of environmental air influences the  
496 convective activity by affecting temperature/moisture and buoyancy of convective parcel.  
497 Therefore, Song and Zhang (2018) extended the ZM scheme to a spectral cloud model that  
498 explicitly describes every type of convective elements in ZM scheme, in which the lateral  
499 entrainment rate varies vertically depending on the buoyancy and updraft velocity following  
500 Gregory (2001). In addition, the CAPE-based closure in the original ZM scheme was also replaced  
501 with a CAPE-generation-based closure as in Zhang and Wang (2006).

502         The simulations with the modified ZM scheme show that the double ITCZ bias is largely  
503 eliminated in the CESM1.2.1. Fig. 10 presents the precipitation distribution from the Global  
504 Precipitation Climatology Project (GPCP) observation (Adler et al., 2003), and simulations of  
505 standard CESM1.2.1 (CTL) and CESM1.2.1 with the new ZM convection scheme (NZM) of Song  
506 and Zhang (2018). In boreal winter (DJF), the standard CESM1.2.1 shows a typical double ITCZ

507 bias in the tropical Pacific, with two parallel bands of intense precipitation ( $>3 \text{ mm day}^{-1}$ )  
508 straddling the equator across the tropical Pacific. In contrast, the simulation with the new ZM  
509 convection scheme successfully reproduces the observed asymmetry between the zonal northern  
510 ITCZ and southeastward SPCZ around the equator. The spurious rain band in the southeastern  
511 Pacific between  $80^\circ\text{W}$  and  $120^\circ\text{W}$  is completely eliminated. The meridional correlation of zonally-  
512 averaged precipitation over  $80^\circ\text{W}$ - $160^\circ\text{W}$  is 0.92 between GPCP and NZM in equatorial region  
513 ( $10^\circ\text{S}$ - $10^\circ\text{N}$ ), which is a significant improvement compared to the correlation of 0.56 between  
514 GPCP and CTL. In boreal summer (JJA), the standard CESM1.2.1 still produces overly-intense  
515 zonal rain band between  $5^\circ$ - $10^\circ\text{S}$  and  $160^\circ\text{E}$ - $120^\circ\text{W}$ , resulting in a large double ITCZ bias in  
516 western and central Pacific. The meridional correlation of zonally-averaged precipitation over  
517  $120^\circ\text{W}$ - $160^\circ\text{E}$  between GPCP and CTL is 0.82 in the equatorial region. With the modified  
518 convection scheme, the zonal rain band in  $5^\circ$ - $10^\circ\text{S}$  and  $120^\circ\text{W}$ - $160^\circ\text{E}$  is almost entirely eliminated,  
519 resulting in the meridional correlation of zonally-averaged precipitation over  $120^\circ\text{W}$ - $160^\circ\text{E}$  with  
520 the GPCP increased to 0.98. The impact of modified convection scheme on double ITCZ bias in  
521 boreal spring (fall) is similar to that in winter (summer) and is not shown. The elimination of the  
522 double ITCZ bias through modification of convection parameterization is consistent with a recent  
523 study by Xiang et al. (2017) that concludes that the root of double ITCZ biases lies in the tropics  
524 and subtropics.

525         Accompanying the elimination of the double ITCZ bias, the SST simulation in the eastern  
526 equatorial Pacific is also improved. Fig. 11 shows the annual cycle of SST anomalies averaged  
527 over  $5^\circ\text{S}$ - $5^\circ\text{N}$  from the annual mean in each longitude in equatorial Pacific similar to Fig. 2 of  
528 Mechoso et al. (1995). The observed annual cycle of SST is well captured in both simulations with  
529 and without the double ITCZ. However, the one without double ITCZ (NZM) simulates timing of

530 the warm and cold phases of the cold tongue better. In the CTL run, the warm phase peaks a month  
531 too late and the cold phase peaks about a month too early. From August to December, large cold  
532 anomalies in the CTL run expands westward to as far as the dateline, whereas in both ICOADS  
533 observations and the NZM run they are confined to east of 150°W. On the other hand, SST  
534 anomalies near the dateline are exaggerated in the NZM simulation compared to observations and  
535 CTL.

536 In summary, convective parameterization in AGCMs plays an important role in simulating  
537 ITCZ precipitation distribution. The mechanisms through which it works to form a double ITCZ  
538 or eliminate a double ITCZ in CGCMs involve a complex chain of interactions both within the  
539 atmosphere and through atmosphere-ocean coupling. Within the atmosphere, convection interacts  
540 with large-scale circulation. In a coupled system, the atmospheric circulation affects SST, upper  
541 ocean circulation, and ocean heat transport, which in turn feed back to modulate convection. By  
542 properly designing a convective scheme, as in the case of Song and Zhang (2018), double ITCZ  
543 can be eliminated in all seasons. Thus, it is probably safe to conclude that convective  
544 parameterization in AGCMs is likely the main culprit of the double ITCZ problem in CGCMs.

## 545 **5. Summary and discussions**

546 This study attempts to provide a brief review of the double ITCZ problem in coupled ocean-  
547 atmosphere GCMs and progress made over the last two decades. It is not intended to be exhaustive  
548 and cover everything in the subject area, but rather to focus on problem areas that are believed to  
549 be major contributors to double ITCZ in GCMs. These include 1) negative biases in simulations  
550 of southeastern Pacific marine boundary layer stratus clouds and associated warm SST biases, 2)  
551 negative biases in Southern Ocean clouds and excessive absorption of shortwave radiation in



552 southern hemisphere, and 3) convective parameterization in atmospheric GCMs and coupled  
553 ocean-atmosphere feedbacks.

554         The southeastern Pacific low-levels clouds are seriously under-simulated in all AGCMs,  
555 and remain so even in the latest models. As a result, SSTs underneath the clouds are higher, which  
556 produce weakened southeasterly winds that in turn produce a weaker ocean upwelling near the  
557 Peruvian coast. When this patch of relatively warm water is advected westward by the south  
558 equatorial current, warm SST biases propagate westward to the eastern and central equatorial  
559 Pacific south of the equator, promoting convection in these regions, thereby forming a spurious  
560 double ITCZ. Earlier coupled model experiments by Ma et al. (1996) support this feedback  
561 mechanism between subtropical stratus clouds and ITCZ biases. When they prescribe southeastern  
562 Pacific cloud deck in the atmospheric model, positive SST biases in the region as well as regions  
563 downstream of the ocean currents are reduced. So are the double ITCZ. However, the cold tongue  
564 simulation over the equator is degraded. Going a step further, Song and Zhang (2016, 2017)  
565 prescribed SST in southeastern Pacific, tropical North Atlantic or both in a CGCM. Similar to Ma  
566 et al. (1996), they also found that the double ITCZ problem was alleviated to some extent. Therefore,  
567 the poor simulation of southeastern Pacific marine stratus clouds is only a contributing factor to  
568 the double ITCZ problem.

569         In recent years, searching for links between the double ITCZ problem and model biases in  
570 extratropics has become very active. This largely stems from theoretical energetics analysis of  
571 inter-hemispheric heat transport and diagnostic analysis of CMIP5 models. Recognizing high  
572 correlations among cross-equatorial atmospheric energy transport, extratropical shortwave cloud  
573 absorption asymmetry and the ITCZ position in CMIP5 models, Hwang and Frierson (2013)  
574 proposed a mechanism linking double ITCZ biases to shortwave absorption biases in Southern

575 Ocean. It goes as the following: The excess energy received over the Southern Ocean due to  
576 negative cloud biases must be exported to the northern hemisphere through enhanced Hadley  
577 circulation. This requires the ascending branch of the Hadley cell, i.e. the ITCZ, to move to the  
578 south of the equator, resulting in a double ITCZ. However, subsequent coupled model experiments  
579 by Kay et al. (2016), Hawcroft et al. (2017, 2018) and Green and Marshall (2017), as well  
580 theoretical work by Schneider (2017) indicate that the majority (70 to 80%) of the required energy  
581 transport is accomplished through ocean circulation, and atmospheric transport only plays a  
582 secondary role. Therefore, based on these studies it appears that double ITCZ is not related to  
583 extratropical biases over the Southern Ocean. However, one exception is the work by Machoso et  
584 al. (2016), which finds that the ITCZ position in a CGCM (UCLA GCM) responds strongly to  
585 energy perturbation in the southern extratropics via strong coupling among subtropical marine  
586 stratus clouds, southeasterly trade winds and SST. Further research along this line could offer new  
587 insight into the role of the Southern Ocean energy perturbation in ITCZ biases.

588         Precipitation in the ITCZ is of convective nature. Thus, convective parameterization has  
589 long been suspected to be the cause of double ITCZ. A number of factors in convection and other  
590 moist physics parameterization schemes have been examined in efforts to address the double ITCZ  
591 problem in both AGCMs and CGCMs. However, progress has been slow. Changing closure  
592 assumptions from CAPE-based to large-scale CAPE generation based in the ZM scheme was able  
593 to eliminate double ITCZ in warm season (June-November) in the NCAR CCSM3 (Zhang and  
594 Wang 2006). Rain re-evaporation and coupling between precipitation and planetary boundary  
595 layer convergence were also identified as an important process in double ITCZ formation in an  
596 AGCM (Bacmeister et al. 2007). Similarly, entrainment of dry air into convective updrafts and its  
597 interaction with environment humidity were also found important in ITCZ simulation (Oueslati

598 and Bellon 2013). The recent work by Song and Zhang (2018) showed that improving the trigger  
599 function, convective updraft model, entrainment rates and closure in the ZM scheme eliminated  
600 the double ITCZ bias in all four seasons in the NCAR CESM1. The development of double ITCZ  
601 involves a chain of complex interactions among convection, atmospheric large-scale circulation,  
602 SST, surface turbulent fluxes, and upper ocean circulation and heat transport. The modified  
603 convective parameterization is able to break this chain of interaction, thereby stopping the  
604 development of the double ITCZ.

605         The double ITCZ problem has plagued generations of global climate models and Earth  
606 system models. Tian (2015) showed that the equilibrium climate sensitivity is closely related to  
607 ITCZ simulation in CMIP5 models: the larger the double ITCZ bias, the smaller the equilibrium  
608 climate sensitivity. Zhou and Xie (2015) found that climatological model biases such as double  
609 ITCZ can seriously affect the future project of tropical climate change. Therefore, improved  
610 simulations of ITCZ will have important ramifications in climate change research. Since double  
611 ITCZ is a result of complex coupled feedbacks involving many atmospheric and oceanic processes,  
612 the same convection parameterization scheme that eliminates double ITCZ in one model may not  
613 be able to produce the same effect in a different model. Because of this, improving ITCZ  
614 simulation sounds like a hit or miss. However, recently Xiang et al. (2017) developed a diagnostic  
615 relationship to predict the severity of double ITCZ in coupled models using atmospheric model  
616 simulations from CMIP5. They found that biases in interhemispheric asymmetry averaged over  
617 tropical and subtropical regions of net surface heat flux or top-of-atmosphere shortwave radiation  
618 in AGCMs are good predictors of double ITCZ biases in CGCMs. If this is true, it should be a  
619 powerful tool for model development efforts, as it can identify the potential of double ITCZ  
620 problem without expensive coupled model integrations of a model.

621

622

623 *Acknowledgments:* This material is based upon work supported by the U.S. Department of Energy,  
624 Office of Science, Biological and Environmental Research Program, under Awards DE-  
625 SC0019373 and DE-SC0016504, and the National Science Foundation Grant AGS-1549259. YW  
626 was supported by the National Key Research and Development Program of China Grant  
627 2017YFA0604000. The authors thank Professor Roberto Mechoso for offering his insight into the  
628 ITCZ problem and for his valuable suggestions to improve the manuscript. They also thank an  
629 anonymous reviewer for his/her constructive comments. GJZ thanks Fengfei Song for reproducing  
630 Figures 3 and 4 for him.

631

632 **References:**

- 633 Adler, R.F. *et al.*, The Version-2 Global Precipitation Climatology Project (GPCP) Monthly  
634 Precipitation Analysis (1979–Present), *Journal of Hydrometeorology* **4**(2003), pp. 1147-  
635 1167.
- 636 Bacmeister, J.T., Suarez, M.J., Robertson, F.R., Rain Reevaporation, Boundary Layer–Convection  
637 Interactions, and Pacific Rainfall Patterns in an AGCM, *Journal of the Atmospheric*  
638 *Sciences* **63**(2006), pp. 3383-3403.
- 639 Bellucci, A., S. Gualdi, and A. Navarra, 2010, Double-ITCZ syndrome in coupled general  
640 circulation models: The role of large-scale vertical circulation regimes. *J. Climate*, **23**,  
641 1127-1145.
- 642 Bony, S., J. L. Dufresne, H. Le Treut, J. J. Morcrette, and C. Senior, 2004: On dynamic and  
643 thermodynamic components of cloud changes. *Climate Dyn.*, **22**, 71–86.
- 644 Chao, W.C., Chen, B., Multiple Quasi Equilibria of the ITCZ and the Origin of Monsoon Onset.  
645 Part II: Rotational ITCZ Attractors, *Journal of the Atmospheric Sciences* **58**(2001), pp.  
646 2820-2831.
- 647 de Rooy, W.C. *et al.*, Entrainment and detrainment in cumulus convection: an overview, *Quarterly*  
648 *Journal of the Royal Meteorological Society* **139**(2013), pp. 1-19.
- 649 Green, B., Marshall, J., Coupling of Trade Winds with Ocean Circulation Damps ITCZ Shifts,  
650 *Journal of Climate* **30**(2017), pp. 4395-4411.
- 651 Gregory, D., Estimation of entrainment rate in simple models of convective clouds, *Quarterly*  
652 *Journal of the Royal Meteorological Society* **127**(2001), pp. 53-72.
- 653 Hawcroft, M. *et al.*, Southern Ocean albedo, inter-hemispheric energy transports and the double  
654 ITCZ: Global impacts of biases in a coupled model, *Clim Dyn* **48**(2017), pp. 2279-2295.
- 655 Hawcroft, M., J. M. Haywood, M. Collins, and A. Jones, The contrasting climate response to  
656 tropical and extratropical energy perturbations, *Clim Dyn*, **49**(2018), pp. 3231-3249.
- 657 Hwang, Y.-T., Frierson, D.M.W., Link between the double-Intertropical Convergence Zone  
658 problem and cloud biases over the Southern Ocean, *Proceedings of the National Academy*  
659 *of Sciences*(2013), 110, pp.4935–4940, doi:10.1073/pnas.1213302110.
- 660 Kang, S.M., Held, I.M., Frierson, D.M.W., Zhao, M., The Response of the ITCZ to Extratropical  
661 Thermal Forcing: Idealized Slab-Ocean Experiments with a GCM, *Journal of Climate*  
662 **21**(2008), pp. 3521-3532.

663 Kang, S.M., Frierson, D.M.W., Held, I.M., The Tropical Response to Extratropical Thermal  
664 Forcing in an Idealized GCM: The Importance of Radiative Feedbacks and Convective  
665 Parameterization, *Journal of the Atmospheric Sciences* **66**(2009), pp. 2812-2827.

666 Kay, J.E. *et al.*, Global Climate Impacts of Fixing the Southern Ocean Shortwave Radiation Bias  
667 in the Community Earth System Model (CESM), *Journal of Climate* **29**(2016), pp. 4617-  
668 4636.

669 Lin, J.-L., The Double-ITCZ Problem in IPCC AR4 Coupled GCMs: Ocean–Atmosphere  
670 Feedback Analysis, *Journal of Climate* **20**(2007), pp. 4497-4525.

671 Ma, C.-C., Mechoso, C.R., Robertson, A.W., Arakawa, A., Peruvian Stratus Clouds and the  
672 Tropical Pacific Circulation: A Coupled Ocean-Atmosphere GCM Study, *Journal of*  
673 *Climate* **9**(1996), pp. 1635-1645.

674 Mechoso, C.R. *et al.*, The Seasonal Cycle over the Tropical Pacific in Coupled Ocean–Atmosphere  
675 General Circulation Models, *Monthly Weather Review* **123**(1995), pp. 2825-2838.

676 Mechoso, C.R. *et al.*, Can reducing the incoming energy flux over the Southern Ocean in a CGCM  
677 improve its simulation of tropical climate?, *Geophysical Research Letters* **43**(2016), pp.  
678 11,057-011,063.

679 Oueslati, B., Bellon, G., Convective Entrainment and Large-Scale Organization of Tropical  
680 Precipitation: Sensitivity of the CNRM-CM5 Hierarchy of Models, *Journal of Climate*  
681 **26**(2013), pp. 2931-2946.

682 Oueslati, B., Bellon, G., 2015: The double ITCZ bias in CMIP5 models: Interaction between SST,  
683 large-scale circulation and precipitation. *Clim. Dyn.*, **44**, 585-607.

684 Schneider, T., Feedback of Atmosphere-Ocean Coupling on Shifts of the Intertropical  
685 Convergence Zone, *Geophysical Research Letters* **44**(2017), pp. 11,644-611,653.

686 Song, F., Zhang, G.J., Effects of Southeastern Pacific Sea Surface Temperature on the Double-  
687 ITCZ Bias in NCAR CESM1, *Journal of Climate* **29**(2016), pp. 7417-7433.

688 Song, F., Zhang, G.J., Impact of Tropical SSTs in the North Atlantic and Southeastern Pacific on  
689 the Eastern Pacific ITCZ, *Journal of Climate* **30**(2017), pp. 1291-1305.

690 Song, X., Zhang, G.J., Convection Parameterization, Tropical Pacific Double ITCZ, and Upper-  
691 Ocean Biases in the NCAR CCSM3. Part I: Climatology and Atmospheric Feedback,  
692 *Journal of Climate* **22**(2009), pp. 4299-4315.

693 Song, X., Zhang, G.J., The Roles of Convection Parameterization in the Formation of Double  
694 ITCZ Syndrome in the NCAR CESM: I. Atmospheric Processes, *Journal of Advances in*  
695 *Modeling Earth Systems* **10**(2018), pp. 842-866.

696 Song, X., Zhang, G.J., Culprit of the eastern Pacific double ITCZ bias in the NCAR CESM1.2,  
697 *Journal of Climate* (under revision).

698 Suhas, E., Zhang, G.J., Evaluation of Trigger Functions for Convective Parameterization Schemes  
699 Using Observations, *Journal of Climate* **27**(2014), pp. 7647-7666.

700 Wang, C., Zhang, L., Lee, S.-K., Wu, L., Mechoso, C.R., A global perspective on CMIP5 climate  
701 model biases, *Nature Climate Change* **4**(2014), p. 201.

702 Xiang, B., M. Zhao, I. M. Held, and J.-C. Golaz, Predicting the severity of spurious “double ITCZ”  
703 problem in CMIP5 coupled models from AMIP simulations, *Geophys. Res. Lett.*, **44**(2017),  
704 pp. 1520–1527, doi:10.1002/2016GL071992.

705 Xie, P.-P., and P. Arkin, Global Precipitation: A 17-Year Monthly Analysis Based on Gauge  
706 Observations, Satellite Estimates and Numerical Model Outputs. doi: 10.1175/1520-  
707 0477(1997) *Bull. Amer. Meteor. Soc.* **78**, 2539–2558, 1997.

708 Xie, S.-P., Philander, S.G.H., A coupled ocean-atmosphere model of relevance to the ITCZ in the  
709 eastern Pacific, *Tellus A* **46**(1994), pp. 340-350.

710 Yu, J.-Y., Mechoso, C.R., Links between Annual Variations of Peruvian Stratocumulus Clouds  
711 and of SST in the Eastern Equatorial Pacific, *Journal of Climate* **12**(1999), pp. 3305-3318.

712 Zhang, C., Double ITCZs, *Journal of Geophysical Research: Atmospheres* **106**(2001), pp. 11785-  
713 11792.

714 Zhang, G.J., Convective quasi-equilibrium in midlatitude continental environment and its effect  
715 on convective parameterization, *Journal of Geophysical Research: Atmospheres*  
716 **107**(2002), pp. ACL 12-11-ACL 12-16.

717 Zhang, G.J., McFarlane, N.A., Sensitivity of climate simulations to the parameterization of  
718 cumulus convection in the Canadian Climate Centre general circulation model,  
719 *Atmosphere-Ocean* **33**(1995), pp. 407-446.

720 Zhang, G.J. and M. Mu, Effects of modifications to the Zhang-McFarlane convection  
721 parameterization on the simulation of the tropical precipitation in the National Center for  
722 Atmospheric Research Community Climate Model, version 3. *J. Geophys. Res.*, **110**,  
723 **D09109** (2005), doi:10.1029/2004JD005617.

724 Zhang, G.J., Song, X., Convection Parameterization, Tropical Pacific Double ITCZ, and Upper-  
725 Ocean Biases in the NCAR CCSM3. Part II: Coupled Feedback and the Role of Ocean  
726 Heat Transport, *Journal of Climate* **23**(2010), pp. 800-812.

727 Zhang, G.J., Wang, H., Toward mitigating the double ITCZ problem in NCAR CCSM3,  
728 *Geophysical Research Letters* **33**(2006).

729 Zhang, G.J., Wu, X., Zeng, X., Mitovski, T., Estimation of convective entrainment properties from  
730 a cloud-resolving model simulation during TWP-ICE, *Clim Dyn* **47**(2016), pp. 2177-2192.

731 Zhang, L., C. Wang, Z. Song, and S.-K. Lee, Remote effect of the model cold bias in the tropical  
732 North Atlantic on the warm bias in the tropical southeastern Pacific, *J. Adv. Model. Earth*  
733 *Syst.*, **6**(2014), pp. 1016–1026, doi:10.1002/2014MS000338.

734 Zhang, X., W. Lin, and M. Zhang, Toward understanding the double Intertropical Convergence  
735 Zone pathology in coupled ocean-atmosphere general circulation models, *J. Geophys. Res.*,  
736 **112**(2007), D12102, doi:10.1029/2006JD007878.

737 Zhang, X., Liu, H., Zhang, M., Double ITCZ in Coupled Ocean-Atmosphere Models: From  
738 CMIP3 to CMIP5, *Geophysical Research Letters* **42**(2015), pp. 8651-8659.

739 Zhou, Z.-Q., and S.-P. Xie, Effects of climatological model biases on the projection of tropical  
740 climate change, *Journal of Climate*, **28**(2015), pp. 9909-9917. DOI: 10.1175/JCLI-D-15-  
741 0243.1

742  
743  
744



745 **Figure Captions:**

746 Fig. 1: Tropical precipitation distribution from a) GPCP observations (1985-2004) and b) ensemble  
747 mean of CMIP5 model simulations. South of the equator precipitation from CMIP5 models  
748 shows a clear double ITCZ in central and eastern Pacific.

749 Fig. 2: Observed low cloud fraction from CALIPSO and shortwave cloud radiative forcing from  
750 CERES-EBAF and corresponding AMIP simulations from CMIP5 models in southeast  
751 Pacific marine stratus region.

752 Fig. 3: Annual-mean precipitation (units: mm/day) in (a) GPCP observations, (c) CNTL run, (e)  
753 SEP run, and the differences between (b) CNTL run and GPCP, (d) SEP run and GPCP, and  
754 (f) SEP run and CNTL run. Stippled regions in (f) indicate precipitation differences exceeding  
755 5% significance level (adopted from Song and Zhang, 2016).

756 Fig. 4: Boreal spring-mean difference between TNA and CTL simulations for a) SST (shaded;  
757 units: °C) and 925 hPa wind (vectors; units: m/s) and (b) precipitation (mm/day), (modified  
758 from Song and Zhang, 2017).

759 Fig. 5: Schematic showing climate response to absorbed shortwave radiation bias reduction (less  
760 shortwave absorption in Southern Ocean, more shortwave absorption in the tropics) (a) with  
761 fixed ocean heat transport and (b) with dynamic ocean heat transport. All indicated changes  
762 are anomalies relative to a mean state climate (adopted from Kay et al., 2016).

763 Fig. 6: Global distribution of precipitation for June-July-August (JJA) for (a) standard CCSM3  
764 (CTRL), (b) CCSM3 with modified convection parameterization (ICON), and (c) Xie-Arkin  
765 observations. The model results are for 10-yr average (adopted from Zhang and Wang, 2006).

766 Fig. 7: Time series of 22-year-long model integrations for (a) precipitation, (b) SST, and (c)  
767 shortwave cloud forcing averaged over (10 °S-5 °S, 180 °-130 °W). Solid line is for ICON and

768 dashed line is for CTRL. For the first 11 years, CTRL uses the original ZM scheme with CAPE-  
769 based closure and ICON uses a revised closure. At the end of year 11, the closures are swapped  
770 between the two runs.

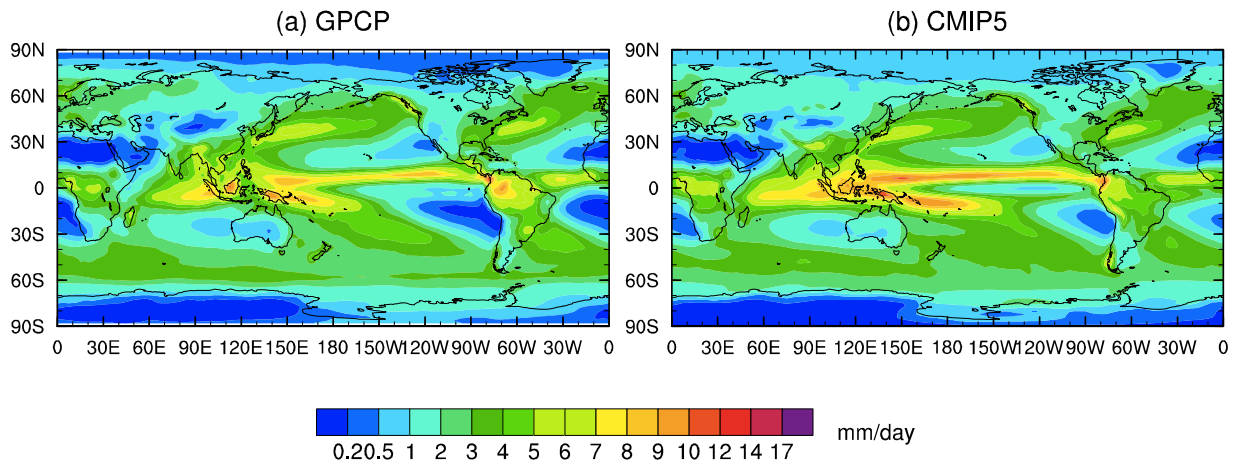
771 Fig. 8: Schematic depicting (a) the formation and (b) suppression mechanisms of double ITCZ  
772 bias in central Pacific with modified convection scheme. The solid and dashed orange lines  
773 denote the Walker circulation and the secondary circulation induced by convection,  
774 respectively. The wind barbs denote surface easterly wind with size representing its strength.  
775 The black curved arrow denotes surface wind stress curl, and the blue wiggly arrows denote  
776 surface evaporation with size representing its strength. The region surrounded by red solid  
777 curve in the western part denotes the western Pacific warm pool of SST. The peaks of blue and  
778 black curves denote the ridges of thermocline and sea surface height, respectively. The SECC  
779 and SEC represent the eastward South Equatorial Counter Current and westward South  
780 Equatorial Current, respectively.

781 Fig. 9: Latitude-depth cross section of JJA mean ocean potential temperature (shaded, °C) and  
782 zonal current (white contours, eastward in solid and westward in dashed lines,  $\text{cm s}^{-1}$ ),  
783 averaged over  $180^\circ\text{E}$ - $150^\circ\text{W}$  for (a) CTL, (b) RZM and (c) GODAS (adopted from Zhang  
784 and Song, 2010).

785 Fig. 10: Seasonal mean precipitation rates ( $\text{mm day}^{-1}$ ) from Global Precipitation Climatology  
786 Project (GPCP) observation for (a) DJF and (b) JJA, from standard CESM1.2.1 (CTL) for (c)  
787 DJF and (d) JJA, and from CESM 1.2.1 with a modified convection scheme (NZM) for (e)  
788 DJF and (f) JJA. Averages of the last 5 years of 10-year CESM1.2.1 simulations are shown  
789 (adopted from Song and Zhang, 2018).

790 Fig. 11: Annual cycle of SST anomalies from the annual mean at each longitude in the equatorial  
791 Pacific averaged over 5S-5N for ICOADS observations (left), simulation with the original  
792 ZM convection scheme (CTL, middle) and simulation with modified ZM scheme (NZM,  
793 right).  
794  
795

796  
797  
798  
799  
800  
801  
802

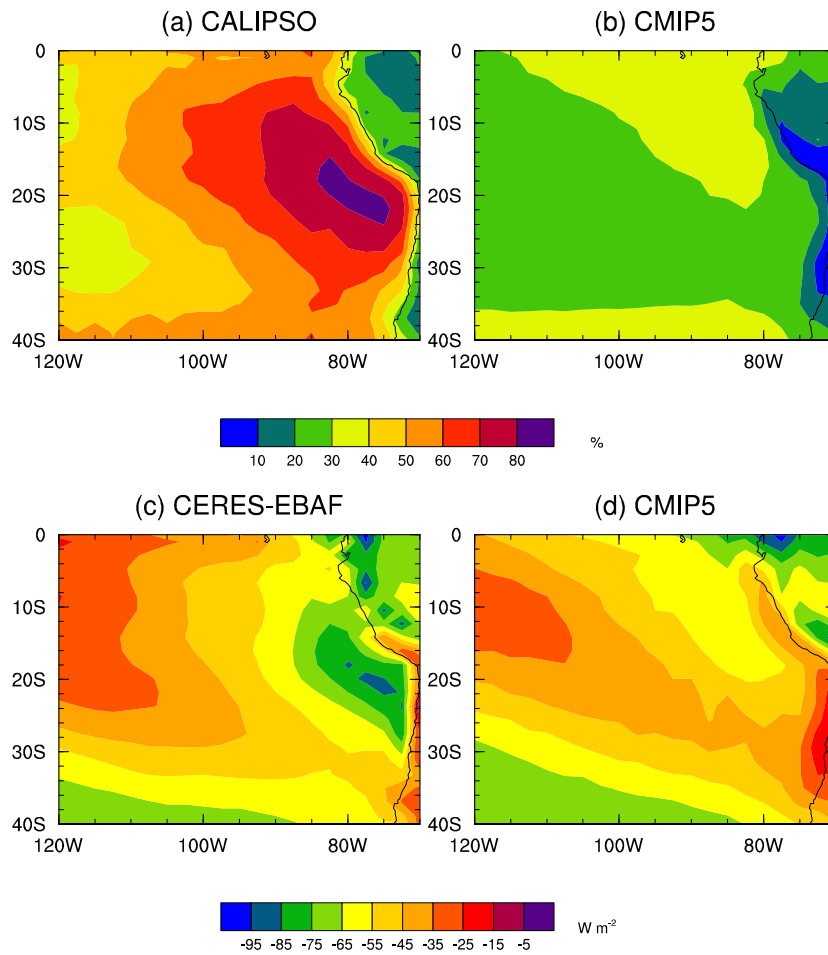


803

804 Fig. 1: Tropical precipitation distribution from a) GPCP observations (1985-2004) and b) ensemble  
805 mean of CMIP5 model simulations. South of the equator precipitation from CMIP5 models shows  
806 a clear double ITCZ in central and eastern Pacific.

807  
808

809  
810  
811  
812

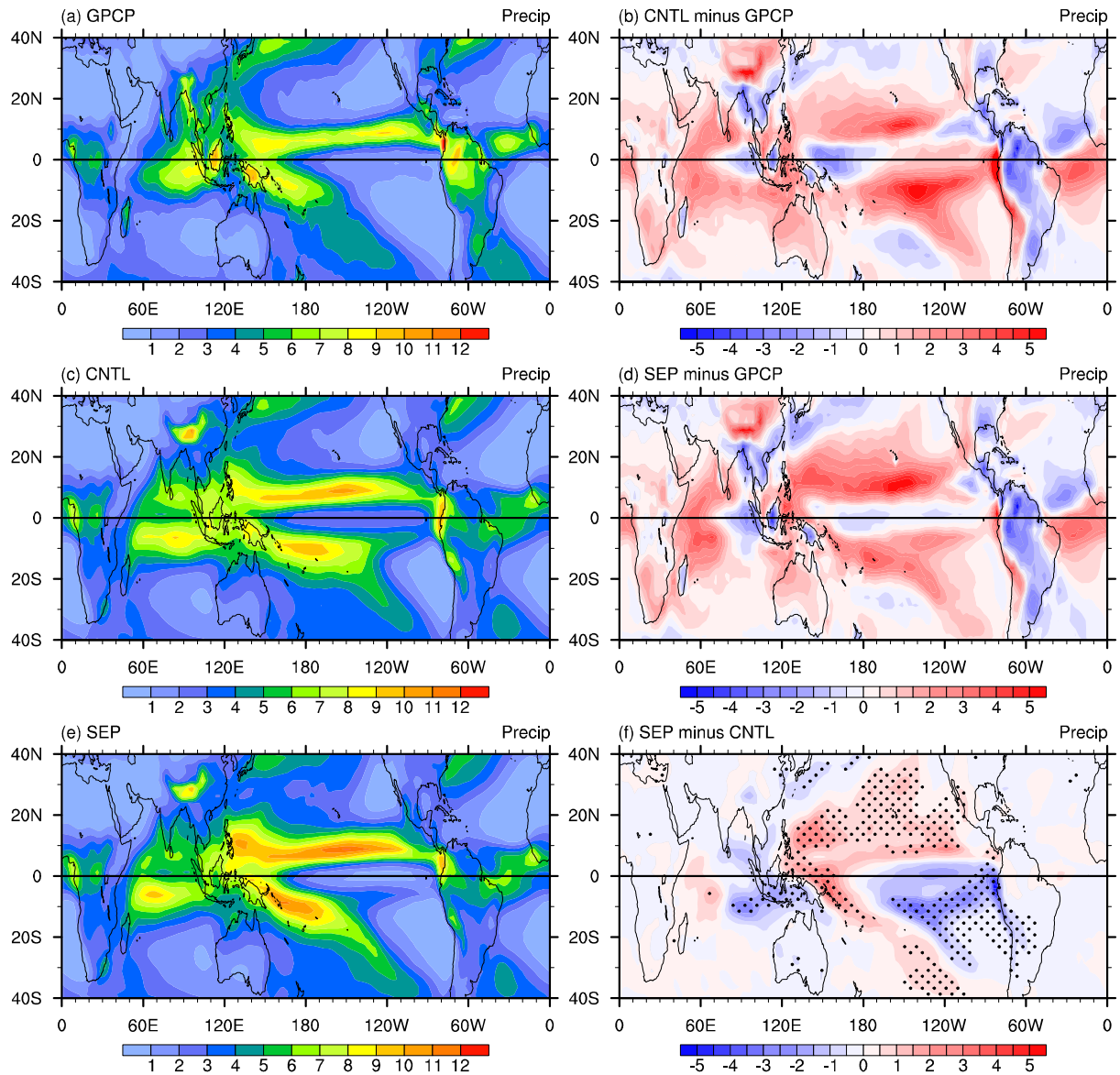


813  
814  
815  
816  
817  
818

Fig. 2: Observed low cloud fraction from CALIPSO and shortwave cloud radiative forcing from CERES-EBAF and corresponding AMIP simulations from CMIP5 models in southeast Pacific marine stratus region.

819

820



821

822 Fig. 3: Annual-mean precipitation (units: mm/day) in (a) GPCP observations, (c) CNTL run, (e)

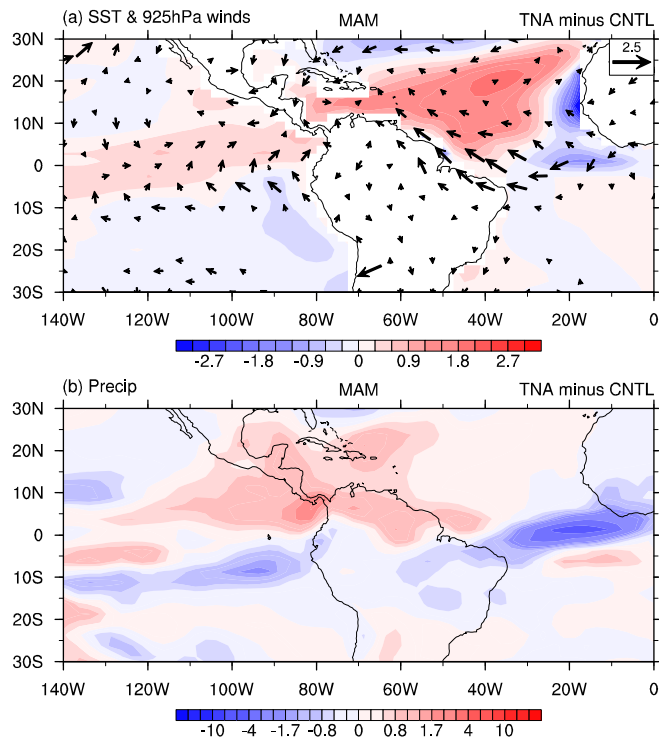
823 SEP run, and the differences between (b) CNTL run and GPCP, (d) SEP run and GPCP, and (f)

824 SEP run and CNTL run. Stippled regions in (f) indicate precipitation differences exceeding 5%

825 significance level (adopted from Song and Zhang, 2016).

826

827



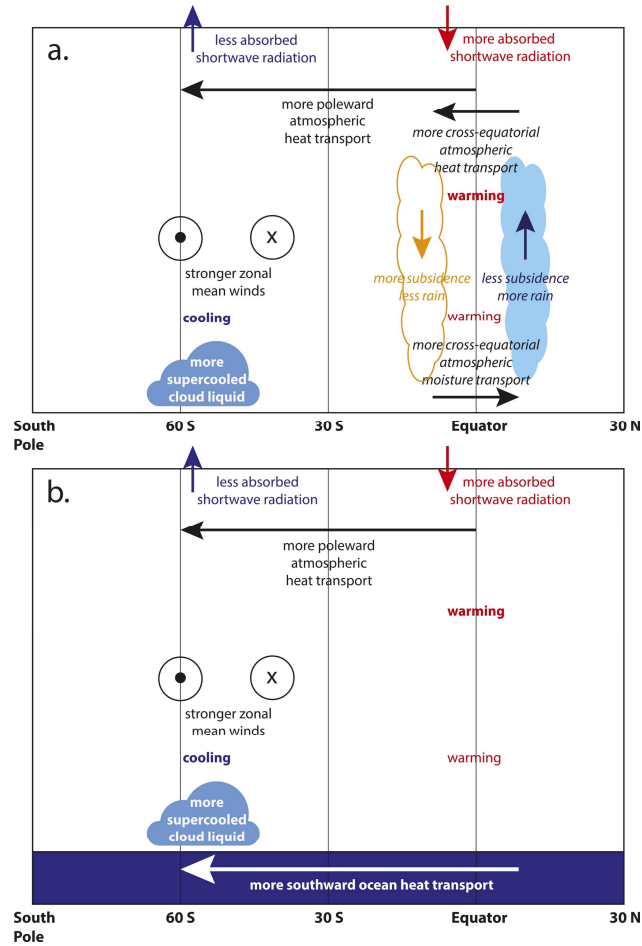
828

829 Fig. 4: Boreal spring-mean difference between TNA and CTL simulations for a) SST (shaded;  
830 units: °C) and 925 hPa wind (vectors; units: m/s) and (b) precipitation (mm/day), (modified from  
831 Song and Zhang, 2017).

832

833

834  
835  
836



837

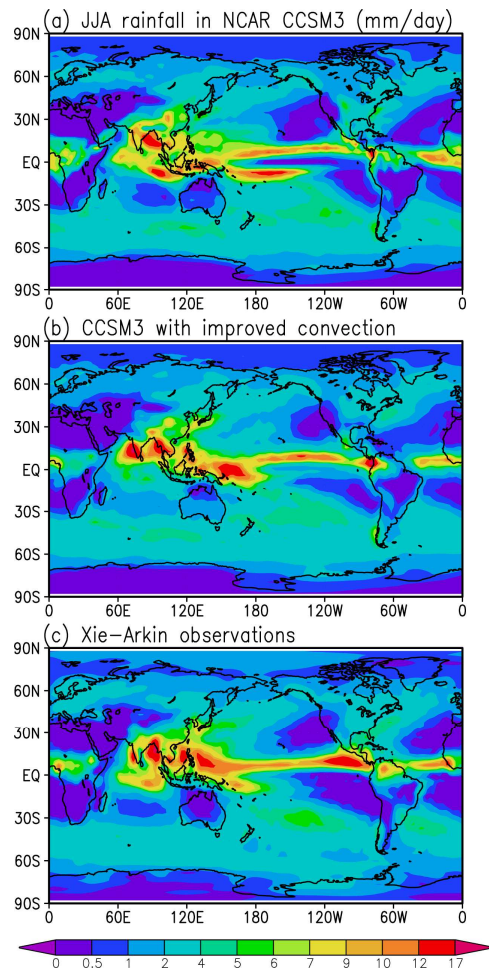
838 Fig. 5: Schematic showing climate response to absorbed shortwave radiation bias reduction (less  
839 shortwave absorption in Southern Ocean, more shortwave absorption in the tropics) (a) with fixed  
840 ocean heat transport and (b) with dynamic ocean heat transport. All indicated changes are  
841 anomalies relative to a mean state climate (adopted from Kay et al., 2016).

842

843



844



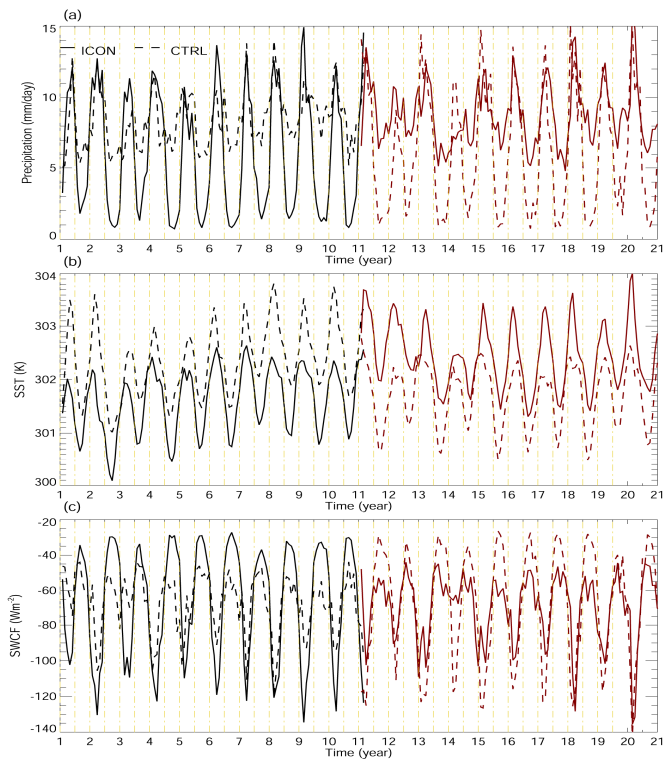
845

846 Fig. 6: Global distribution of precipitation for June-July-August (JJA) for (a) standard CCSM3  
847 (CTRL), (b) CCSM3 with modified convection parameterization (ICON), and (c) Xie-Arkin  
848 observations. The model results are for 10-yr average (adopted from Zhang and Wang, 2006).

849

850

851



852

853 Fig. 7: Time series of 22-year-long model integrations for (a) precipitation, (b) SST, and (c)  
854 shortwave cloud forcing averaged over (10 °S-5 °S, 180 °-130 °W). Solid line is for ICON and  
855 dashed line is for CTRL. For the first 11 years, CTRL uses the original ZM scheme with CAPE-  
856 based closure and ICON uses a revised closure. At the end of year 11, the closures are swapped  
857 between the two runs.

858

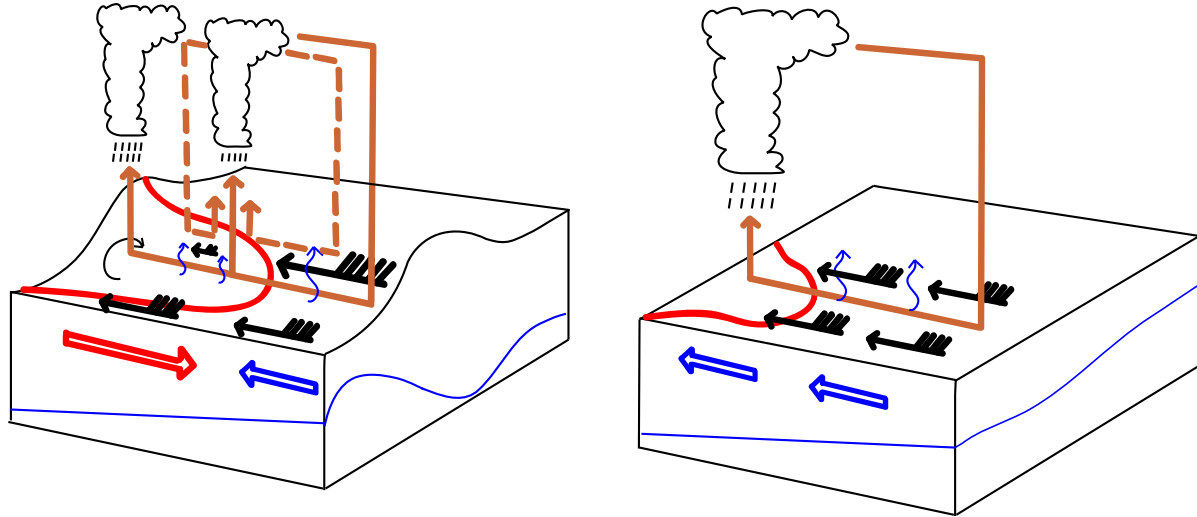
859

860

861

862

863  
864  
865



866  
867

868 Fig. 8: Schematic depicting (a) the formation and (b) suppression mechanisms of double ITCZ

869 bias in the central Pacific with modified convection scheme. The solid and dashed orange lines

870 denote the Walker circulation and the secondary circulation induced by convection, respectively.

871 The wind barbs denote surface easterly wind with size representing its strength. The black curved

872 arrow denotes surface wind stress curl, and the blue wiggly arrows denote surface evaporation

873 with size representing its strength. The region surrounded by red solid curve in the western part

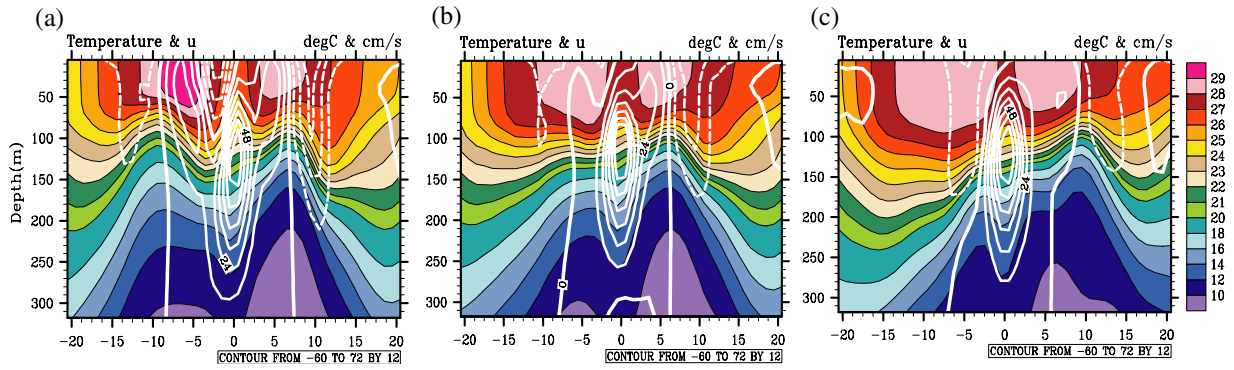
874 denotes the western Pacific warm pool of SST. The peaks of blue and black curves denote the

875 ridges of thermocline and sea surface height, respectively. The SECC and SEC represent the

876 eastward South Equatorial Counter Current and westward South Equatorial Current, respectively.

877  
878

879  
880  
881  
882  
883



884  
885  
886

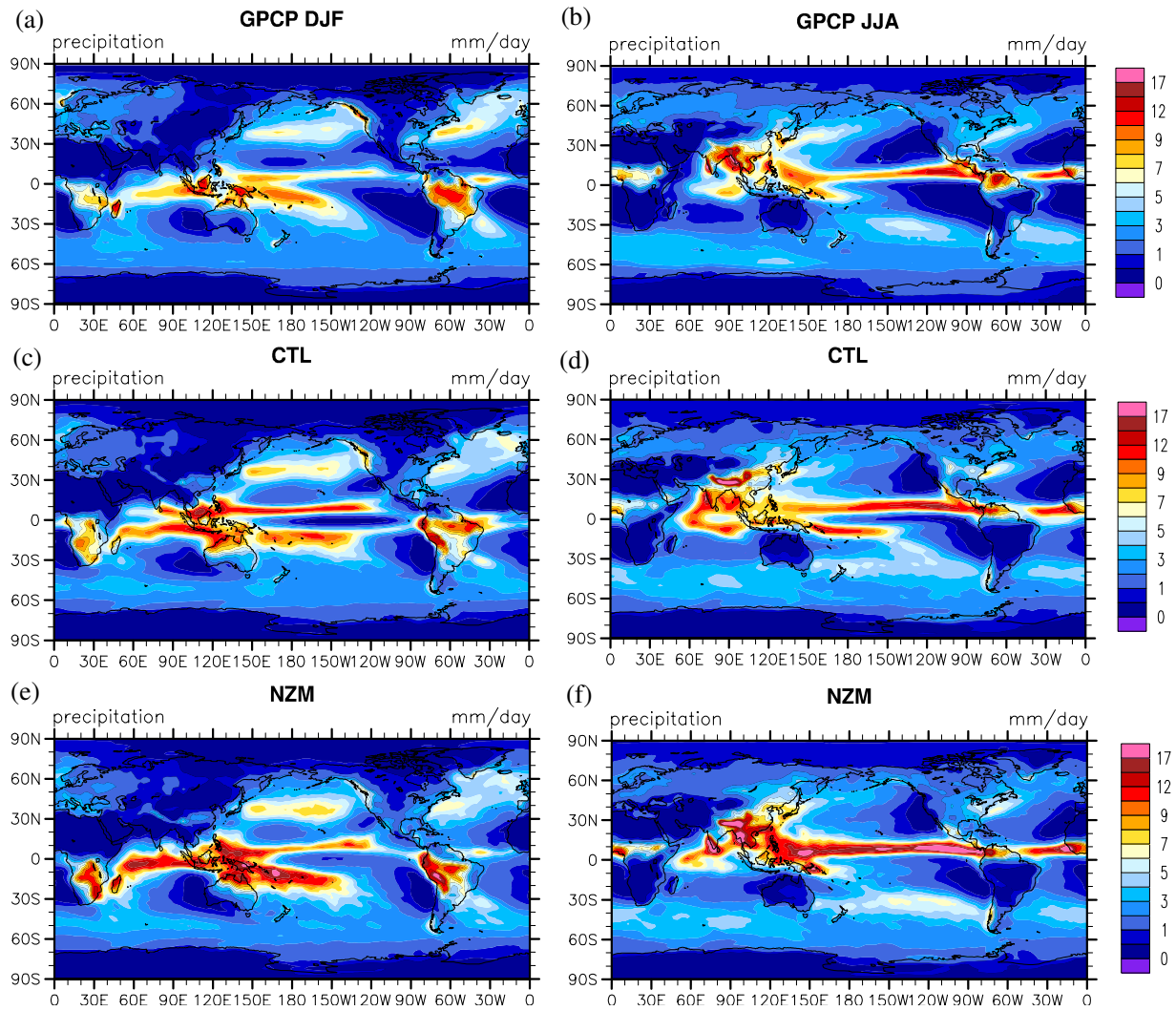
Fig. 9: Latitude-depth cross section of JJA mean ocean potential temperature (shaded, °C) and

zonal current (white contours, eastward in solid and westward in dashed lines,  $\text{cm s}^{-1}$ ), averaged

over 180°E-150°W for (a) CTL, (b) RZM and (c) GODAS (adopted from Zhang and Song,

2010).

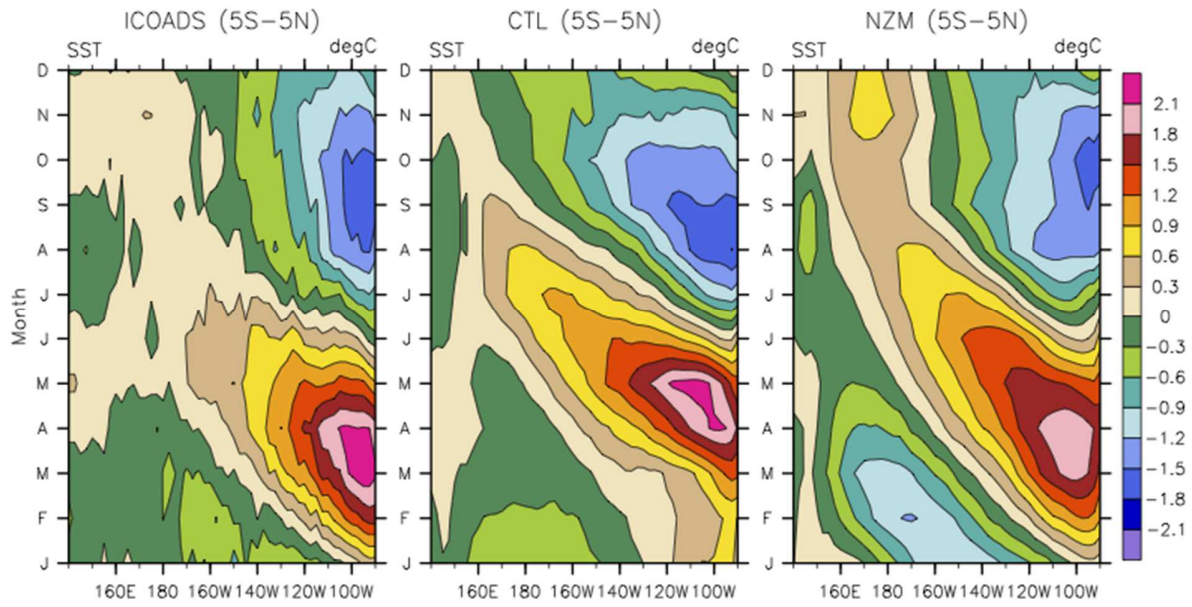
890  
891  
892



893  
 894  
 895 Figure 10: Seasonal mean precipitation rates ( $\text{mm day}^{-1}$ ) from Global Precipitation Climatology  
 896 Project (GPCP) observation for (a) DJF and (b) JJA, from standard CESM1.2.1 (CTL) for (c) DJF  
 897 and (d) JJA, and from CESM 1.2.1 with a modified convection scheme (NZM) for (e) DJF and (f)  
 898 JJA. Averages of the last 5 years of 10-year CESM1.2.1 simulations are shown (adopted from  
 899 Song and Zhang, 2018).

900  
 901  
 902  
 903  
 904  
 905

906  
907  
908



909  
910

911 Fig. 11: Annual cycle of SST anomalies from the annual mean at each longitude in the equatorial  
912 Pacific averaged over 5S-5N for ICOADS observations (left), simulation with the original ZM  
913 convection scheme (CTL, middle) and simulation with modified ZM scheme (NZM, right).